

# BronchusNet: Region and Structure Prior Embedded Representation Learning for Bronchus Segmentation and Classification

Wenhao Huang<sup>1,\*</sup>, Haifan Gong<sup>2,3,\*</sup>, Huan Zhang<sup>1</sup>, Yu Wang<sup>1</sup>,  
Hong Shen<sup>1,#</sup>, Guanbin Li<sup>2,3,#</sup>, Haofeng Li<sup>2,#</sup>

<sup>1</sup> InferVision, <sup>2</sup> Shenzhen Research Institute of Big Data, The Chinese University of Hong Kong (Shenzhen), <sup>3</sup> Sun Yat-sen University

\* denotes equal contribution, # denotes joint corresponding authors.  
shong@infervision.com, liguanbin@mail.sysu.edu.cn, lhaof@foxmail.com

**Abstract.** CT-based bronchial tree analysis plays an important role in the computer-aided diagnosis for respiratory diseases, as it could provide structured information for clinicians. The basis of airway analysis is bronchial tree reconstruction, which consists of bronchus segmentation and classification. However, there remains a challenge for accurate bronchial analysis due to the individual variations and the severe class imbalance. In this paper, we propose a region and structure prior embedded framework named BronchusNet to achieve accurate segmentation and classification of bronchial regions in CT images. For bronchus segmentation, we propose an adaptive hard region-aware UNet that incorporates multi-level prior guidance of hard pixel-wise samples in the general Unet segmentation network to achieve better hierarchical feature learning. For the classification of bronchial branches, we propose a hybrid point-voxel graph learning module to fully exploit bronchial structure priors and to support simultaneous feature interactions across different branches. To facilitate the study of bronchial analysis, we contribute **BRSC**: an open-access benchmark of **BR**onchus imaging analysis with high-quality pixel-wise **S**egmentation masks and the **C**lass of bronchial segments. Experimental results on BRSC show that our proposed method not only achieves the state-of-the-art performance for binary segmentation of bronchial region but also exceeds the best existing method on bronchial branches classification by 6.9%.

**Keywords:** Bronchus Classification · Bronchus Segmentation · Graph Neural Network · Point Cloud · Convolution Neural Network

## 1 Introduction

CT-based lung airway analysis is clinically important as it could provide valuable quantitative information to assist lung disease diagnosis and navigation of surgical [16,10]. Bronchial tree reconstruction is the basis of quantitative lung airway analysis, which usually comprises two steps. The first step is to extract

the whole airway tree mask from the original CT imaging. The second step is to label major anatomical branches based on bronchus classification. The automatic bronchial tree reconstruction can further assist more clinical processes, such as individual airway tree phenotype matching and lung lobe or lung segment classification [8,18]. There still exist two main obstacles: (1) the extreme unbalanced foreground and background in bronchus segmentation; (2) the ignorance of inherent topology or prior knowledge for bronchus segment classification.

Based on the above observations, we propose BronchusNet, a region and structure prior embedded framework to effectively segment and classify the bronchus in CT images. For segmentation task, we design an Adaptive Hard Region-aware UNet (AHR-UNet) to accurately segment the bronchus from the background. The AHR-UNet first uses a prediction screening based method to discover hard region, then highlights the hard region with max-pooling in a coarse-to-fine manner. After that, we follow the inherent topological of the bronchus tree and design a neural network based on Point-Voxel Graph Representation (PVGR) to classify the branches. The idea underlying PVGR is to combine the position information represented by point clouds with the local higher-dimensional convolution features from an additional mask labeling task. Considering the prior knowledge that adjacent segments tend to belong to the same category, a Neighborhood Consistency Regularization is proposed to boost the performance. For evaluation, we manually annotate the airway branch labels of 100 CT scans collected from public datasets and the cooperate hospital. The contribution of this work could be summarized as follows: (1) we have designed a region and structure embedded representation learning framework to segment and classify the bronchus from the lung CT imaging; (2) we propose an Adaptive Hard Region-aware UNet to overcome the extreme imbalance of foreground and background pixel samples during bronchus segmentation training; (3) we contribute a benchmark named BRSC, which contains 100 bronchial cases with accurately pixel-level segmentation mask and anatomical categories. Extensive experimental results on the proposed benchmark showed that BronchusNet significantly exceeds the state-of-the-art methods.

## 2 Related Work

For bronchus segmentation, single-stage networks like U-Net [14], 2.5D net [19], 3D U-Net [3,6,10,12] have been employed, but they often rely on laborious pre/post-processing. Two-stage approaches have shown promising results. Zhao *et al.* [21] used a two-stage 2D+3D U-Net to segment thick and thin bronchus. Qin *et al.* [11] trained an extra model to predict the bronchus connectivity. These methods introduce additional strategies to enhance the segmentation of indistinguishable regions, and cannot achieve end-to-end joint training. Therefore, embedding the hard sample mining module in the network design can exchange the model for the fine segmentation of the bronchial boundary with less amount of parameters.

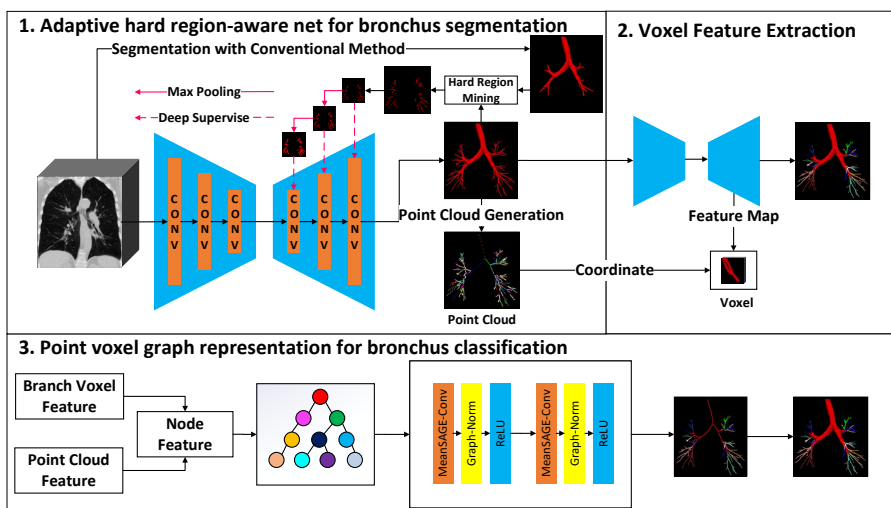


Fig. 1. Overview of the airway segmentation and classification framework.

Bronchus classification remains a challenging task due to the various topology of bronchial trees. Wang et al. [18] achieved lobar-level bronchus classification based on keypoint detection. For deep learning based methods, Zhao et al. [21] applied linear programming to post-process the airway structure predicted by neural models. Nadeem [8] proposed a neural network of two stages that label the lobar-level and segment-level bronchus respectively. Recently, graph-based methods [4,15,20,17] have been studied for the task. Juarez *et al.* [4] replaced the deepest convolutional layer in a U-Net with graph convolutions to improve the airway binary segmentation. However, the previous approaches either require hand-crafted feature [18,21,8] or need additional annotation [17,4], while they are not able to effectively handle the individual variance. Thus, there is a need to develop an efficient and effective framework that can embed both voxel-wise features and point-cloud topology into learnable representations for bronchus classification.

### 3 Method

BronchusNet contains three stages, as shown in Fig. 1. In the first stage, we segment the airways of an input lung CT scans with our Adaptive Hard Region-aware UNet to obtain a 3D binary mask. Secondly, we use a UNet to label the mask and to harvest voxel-wise features for the bronchus. Thirdly, we propose to refine the bronchus classification results based on a Hybrid Point-Voxel Graph.

### 3.1 Adaptive Hard Region-aware UNet

Considering that the bronchial voxels are sparse and scattered, we propose to locate multi-scale hard regions as prior knowledge to guide the representation learning of the bronchial region, and develop an Adaptive Hard Region-aware UNet (ADR-UNet). We first use Otsu’s [9] method to segment the main trachea from the CT imaging, and the hard region  $y_{hr}$  is regarded as the voxels that appear in the ground truth but not in the main trachea. After that, to emphasize the voxels lying on the end of bronchus, we use max-pooling to dilate the area of the hard region  $y_{hr}$ . As the red arrows in Fig. 1 shows, the max-pooling is applied to the hard region for multiple times to synthesize multi-scale supervisions for the decoder of UNet. Formally, the hard region aware loss  $L_{hr}^h$  with respect to the  $h$ -th layer of the decoder is defined as:

$$L_{hr}^h = L_{dice}(pred_{hr}^h, I^h(y_{hr})), \quad (1)$$

where  $pred_{hr}$  and  $y_{hr}$  denote the predicted segmentation of hard region and the hard region of  $h$ -th (from left to right) layer of the decoder, respectively.  $I^h(\cdot)$  denotes the inflation function that max-pools the ground truth with stride 2 for  $h$  times according to the index of the layer.  $L_{dice}$  is the dice loss function. With the hard region aware loss, the final loss function to segment the bronchus is defined as:

$$L_{seg} = \sum_{h=1}^{h=H} L_{hr}^h + L_{dice}, \quad (2)$$

where the  $H$  is the number of layers of the decoder.  $L_{dice}$  is used to supervise the segmentation of the whole airway.

### 3.2 Hybrid Point-Voxel Graph based Representation Learning

We further proposed the point voxel graph neural network to classify the bronchus in a more accurate way. The motivation underlying our framework is that the relative positional information represented by the point cloud helps to overcome the individual variance during the classification process. In the meanwhile, the high-dimension voxel feature could be a strong supplement for bronchus classification as it is able to capture other features of the bronchus such as diameter and direction of the bronchus.

**A. Construction of Bronchial Graph (1) Definition of Node and Edge in the Graph.** Based on the segmentation mask of the bronchus from Stage 1, we construct a Hybrid Point-Voxel Graph with the following steps, as shown in Fig. 2. Firstly, we skeletonize the mask by extracting the centerline (see Fig. 2(b)). Secondly, according to the number  $N$  of foreground voxels in the 26-connected neighborhood of each voxel on the centerline, we define the end-points ( $N = 1$ ), edge-points ( $N = 2$ ), and division-points ( $N \geq 3$ ), as shown in Fig. 2(c). Finally, as Fig. 2(d) shows, we divide the branches into segments (i.e., node in the graph)

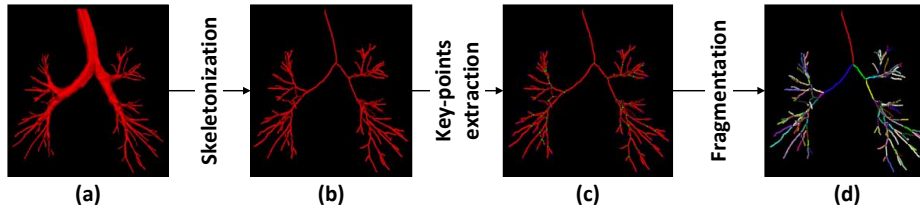


Fig. 2. Workflow for bronchial tree construction.

based on these points. The edge of the graph is defined by the connectivity between line segments, which are divided by a division point.

**(2) Point-wise Coordinate Feature.** To obtain the point-wise coordinate feature, we need to generate the point cloud from the bronchus mask. Based on the bronchus tree shown in Fig. 2(d), we crop out the bounding box from each bronchial segment (i.e., node in the graph) of the bronchus tree. Each segment is composed of centerline’s voxels. Then the coordinate (i.e.,  $X$ ,  $Y$ , and  $Z$ ) of each voxel is normalized to  $[0, 1]$  with respect to the shape of the bounding box. We sub-sample  $K$  voxels on each branch as the number of voxels varies. In this way, we obtain the point cloud feature that contains three-dimensional coordinates of  $K$  voxels with the length  $3 \times K$ .  $K$  is set to 10, empirically.

**(3) Voxel-wise Convolution Feature.** To obtain voxel features, we train a UNet (Stage 2 in Fig. 1) to predict the category of each bronchus branch. A 3D feature map is produced from the penultimate layer of the UNet. We extract  $K$  convolution features from the feature map according to the  $K$  voxel’s coordinate of each bronchial fragment, and aggregate them to a vector of length  $C \times K$ , where  $C$  is the channel of the feature map ( $C = 24$  by default).

**B. Point-Voxel Graph Neural Network** Given the above-defined graph that takes both point cloud features and high-dimension voxel features into account, we design a Point-Voxel Graph Neural Network (PV-GNN) to predict the category of each bronchial segment. The PV-GNN consists of Conv-Norm Blocks and a fully connected layer. The first part of the Conv-Norm Block is Mean Sage-Convolution (MSC) [5], which uses the mean aggregated function to aggregate information from node neighbors to overcome the inductive bias. Considering that the adjacent nodes in the topology of the bronchial tree are relatively sparse, we build up a deep GNN for better information integration in point-clouds. As GNN has a risk of suffering from gradient vanishing as it goes deeper, we introduce Graph Normalization (GN) [2] to shift and scale feature values, which makes graph neural networks converge much faster. Besides the first block, each block is added with element-wise addition which is performed as a residual connection. Let  $H^k$  be the output of the  $k$ -th block and  $\sigma$  refers to ReLU operation, the block is defined as:

$$H^k = \sigma(\text{GN}(\text{MSC}(H^{k-1})) + H^{k-1}). \quad (3)$$

**C. Cross-entropy with Neighborhood Consistency Regularization** Considering the topology of the bronchial tree that the adjacent branches tend to belong to the same category, we design a novel Neighborhood Consistency Regularization (NCR) to penalize local spatial variations and force nearby nodes belonging to the same category to be closer in the latent space. Let  $Y = \{y_1, y_2, \dots, y_N\}$  be the set that contains the one-hot vector of the ground truth of each branch and  $Z = \{z_1, z_2, \dots, z_N\}$  be the set that contains the one-hot vector of model prediction of each branch, the NCR loss is formulated as:

$$L_{NCR} = \frac{\sum_{i=1}^N \sum_j^{V_i} \|z_i - z_j\| \mathbb{I}(y_i = y_j)}{M}, \quad (4)$$

where  $V_i$  is the set of  $i$ 's neighbor and  $j$  is the  $j$ -th node in this set,  $z_i$  denotes the logit vector of node  $i$  from the output of last fully-connection layer,  $\mathbb{I}(\cdot)$  is an indicator function that returns 1 when the condition is met, and returns 0 otherwise, and  $M, N$  are the numbers of edges and nodes in the graph, respectively. Let  $\alpha$  be a scalar to balance the weight of the regularization and CE loss ( $\alpha$  set to 1 empirically.), the overall loss function contains the above NCR and a vanilla Cross-Entropy loss, and can be formulated as:

$$L = L_{CE} + \alpha L_{NCR}. \quad (5)$$

## 4 BRSC: A New Benchmark for Bronchus Segmentation and Classification

We contribute a new benchmark, BRSC, for bronchus segmentation and classification. BRSC contains 100 cases of lung CT images. We collect 60 cases from the currently available database EXACT'09 [7] and LIDC [1]. The remaining 40 cases are collected from our cooperative hospital, which has received the appropriate approvals from the institutional ethical committee. The BRSC benchmark is annotated by two experts with a two-step annotation process. The experts first annotate the airway segmentation, and then label 18 segmental bronchi at the pixel level. Then we mix these data from different sources together and split the dataset into a training set of 70 cases and a test set of 30 cases. To evaluate the performance of the algorithms, we performed the five-fold cross-validation on the training set by randomly selecting 80% data (i.e., 56 cases) for model training and the remaining 20% (i.e., 14 cases) for validation.

## 5 Experiments and Results

**Implementation and Evaluation Details** We use PyTorch 1.10 to build the model, and all models are trained with NVIDIA V100 GPU of 32GB. For bronchus segmentation, we cut the CT imaging into overlapping cubes of shape  $80 \times 80 \times 80$  for training. During inference, We crop a  $64 \times 64 \times 64$  cube from the center of the CT imaging, with  $16 \times 16 \times 16$  overlap between adjacent cubes

**Table 1.** Comparison of bronchus segmentation and classification methods. The best results are shown in **bold**.

Segmentation	Dice-score	Classification	Accuracy	Precision	Recall	F1-score
LP [21]	0.874 $\pm$ 0.02	LP [21]	0.818 $\pm$ 0.01	0.747 $\pm$ 0.01	0.792 $\pm$ 0.02	0.770 $\pm$ 0.02
TS-CNN [20]	0.883 $\pm$ 0.02	TS-NN [8]	0.768 $\pm$ 0.01	0.778 $\pm$ 0.01	0.749 $\pm$ 0.01	0.762 $\pm$ 0.01
SGNet [17]	0.847 $\pm$ 0.02	SGNet [17]	0.856 $\pm$ 0.01	0.850 $\pm$ 0.01	0.844 $\pm$ 0.01	0.847 $\pm$ 0.01
nn-UNet [6]	0.865 $\pm$ 0.01	-	-	-	-	-
BronchusNet	<b>0.912<math>\pm</math>0.01</b>	BronchusNet	<b>0.924<math>\pm</math>0.01</b>	<b>0.923<math>\pm</math>0.01</b>	<b>0.919<math>\pm</math>0.01</b>	<b>0.921<math>\pm</math>0.01</b>

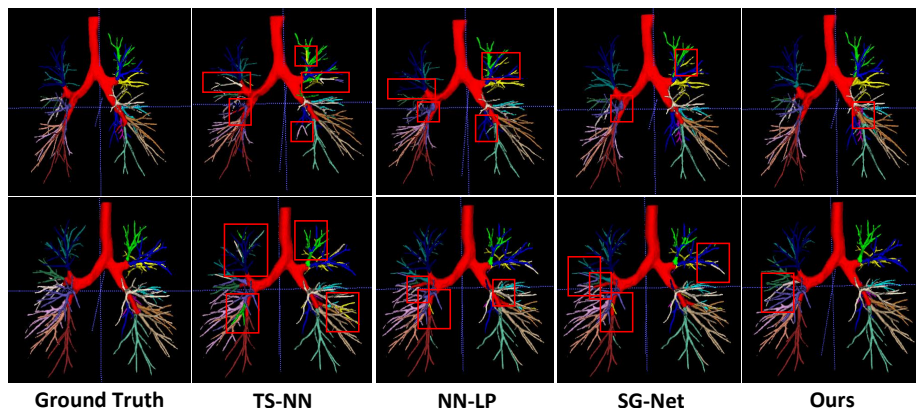


**Fig. 3.** Qualitative analysis on the BRSC benchmark. The misclassified bronchus is bounded by a red box. In the above cases, TS-NN [8] could suffer from errors related to branching variability. LP [21] fails to distinguish the segments with similar angles. SGNet [17] misclassify the thin bronchus while BronchusNet shows robust results.

to avoid prediction of obscure boundary. We train the model for 50 epoches with SGD optimizer and a learning rate of 0.001. Batch size is set to 16. We use Dice score to evaluate the segmentation. For bronchus classification, we augment the training data by applying random affine transform and elastic deformation for 99 times. We use DropEdge [13] for model training to avoid over-fitting. Adam optimizer is applied to train the model with learning rate at 0.001 for 500 epoches, while the batch size is set to 128. The number of layers and hidden dimensions in PV-GNN is set to 5 and 256, respectively. Following [21], we evaluate the classification with the accuracy, precision, recall, and F1-score.

**Comparison with the State-of-the-art** The comparison results for segmentation are shown in the left part of Table 1. Our AHR-UNet significantly outperforms other bronchus segmentation models by taking the hard region prior into account. Specifically, we exceed the previous state-of-the-art TS-CNN by 2.9% w.r.t Dice score. The comparison results for bronchial classification are shown

in the right part of Table. 1. Our models significantly exceed the previous state-of-the-art SGNet by 7.5% on accuracy and 7.7% on F1-score, showing that the hybrid point-voxel graph representation is significantly effective. The qualitative analysis is shown in Fig. 3, the TS-NN [8] under-performance as it only focuses on local features but neglects the global topology of the airway. The hard-crafted feature-based LP [21] fails with segments that have similar angles. The SGNet [17] makes the mistake due to the severe class imbalance. Thanks to the affiliated hard region prior, our BronchusNet is robust to classifying the thin bronchus.

**Ablation study** The ablation study is shown in Table. 2. For segmentation, the UNet with the tailor-designed training strategies shows the competitive result. By taking the hard region into account, our AHR-UNet significantly exceeds the UNet by 3.2% dice score. For classification, “CNN” only uses UNet to label the binary mask, which is underperformance as it could not provide structure prior. “GNN-P” uses the point cloud graph representation to classify the bronchus, which achieves substantial performance improvement (i.e., 6.3%) against the “CNN”. “GNN-PV” takes the voxel-wise convolutional feature into account, which can capture the local texture and the diameter information, thus significantly exceeding the “GNN-P” by 3.8%. “GNN-PVN” embeds the neighborhood consistency regularization into the framework, which brings a performance gain of 1.1%. This result shows that we can better classify the bronchus by using prior knowledge that adjacent segments tend to belong to the same category.

**Table 2.** Ablation study of the bronchus’s segmentation and classification.

Classification Dice score		Segmentation Point Feature Voxel Feature NCR			Accuracy
UNet	0.879 $\pm$ 0.01	CNN			0.819 $\pm$ 0.01
AHR-UNet	0.912 $\pm$ 0.01	GNN-P	✓		0.882 $\pm$ 0.02
-	-	GNN-PV	✓	✓	0.918 $\pm$ 0.01
-	-	GNN-PVN	✓	✓	✓ 0.924 $\pm$ 0.01

## 6 Conclusion

In this paper we present the BronchusNet, a region and structure prior embedded framework for bronchus segmentation and classification. With the tailor-designed adaptive hard region-aware network, the feature representation learning obtains much more accurate bronchus segmentation result. Based on the hybrid point-voxel graph based representation learning, we are able to effectively overcome the individual variance for bronchus segment classification. Additionally, a novel neighbor consistency-based regularization is proposed to boost the performance. We contribute the BRSC benchmark that contains 100 CT scans with pixel-wise masks and segmental-level labels to facilitate future research. The experimental



results on the BRSC benchmark show that our proposed method significantly outperforms the state-of-the-art methods.

## References

1. Armato, S.G., et al.: The lung image database consortium (lidc) and image database resource initiative (idri): a completed reference database of lung nodules on ct scans. *Medical physics* **38**(2), 915–931 (2011)
2. Cai, T., Luo, S., Xu, K., He, D., Liu, T.Y., Wang, L.: Graphnorm: A principled approach to accelerating graph neural network training. In: *ICML* (2021)
3. Charbonnier, J.P., Van Rikxoort, E.M., Setio, A.A., Schaefer-Prokop, C.M., van Ginneken, B., Ciompi, F.: Improving airway segmentation in computed tomography using leak detection with convolutional networks. *Medical image analysis* **36**, 52–60 (2017)
4. Garcia-Uceda Juarez, A., Selvan, R., Saghir, Z., Bruijne, M.d.: A joint 3d unet-graph neural network-based method for airway segmentation from chest cts. In: *International workshop on machine learning in medical imaging*. pp. 583–591. Springer (2019)
5. Hamilton, W.L., Ying, Z., Leskovec, J.: Inductive representation learning on large graphs. In: *NIPS* (2017)
6. Isensee, F., Jaeger, P.F., Kohl, S.A., Petersen, J., Maier-Hein, K.H.: nnu-net: a self-configuring method for deep learning-based biomedical image segmentation. *Nature methods* **18**(2), 203–211 (2021)
7. Lo, P., et al.: Extraction of airways from ct (exact’09). *IEEE transactions on medical imaging* **31**(11), 2093–2107 (2012)
8. Nadeem, S.A.: A fully automated CT-based airway segmentation and branch labeling algorithm using deep learning and conventional image processing. Ph.D. thesis, University of Iowa (2020)
9. Otsu, N.: A threshold selection method from gray-level histograms. *IEEE transactions on systems, man, and cybernetics* **9**(1), 62–66 (1979)
10. Qin, Y., Chen, M., Zheng, H., Gu, Y., Shen, M., Yang, J., Huang, X., Zhu, Y.M., Yang, G.Z.: Airwaynet: a voxel-connectivity aware approach for accurate airway segmentation using convolutional neural networks. In: *International Conference on Medical Image Computing and Computer-Assisted Intervention*. pp. 212–220. Springer (2019)
11. Qin, Y., Gu, Y., Zheng, H., Chen, M., Yang, J., Zhu, Y.M.: Airwaynet-se: A simple-yet-effective approach to improve airway segmentation using context scale fusion. In: *2020 IEEE 17th International Symposium on Biomedical Imaging (ISBI)*. pp. 809–813. IEEE (2020)
12. Qin, Y., Zheng, H., Gu, Y., Huang, X., Yang, J., Wang, L., Yao, F., Zhu, Y.M., Yang, G.Z.: Learning tubule-sensitive cnns for pulmonary airway and artery-vein segmentation in ct. *IEEE Transactions on Medical Imaging* **40**(6), 1603–1617 (2021)
13. Rong, Y., bing Huang, W., Xu, T., Huang, J.: Dropedge: Towards deep graph convolutional networks on node classification. In: *ICLR* (2020)
14. Ronneberger, O., Fischer, P., Brox, T.: U-net: Convolutional networks for biomedical image segmentation. In: *International Conference on Medical image computing and computer-assisted intervention*. pp. 234–241. Springer (2015)

15. Selvan, R., Kipf, T., Welling, M., Juarez, A.G.U., Pedersen, J.H., Petersen, J., de Bruijne, M.: Graph refinement based airway extraction using mean-field networks and graph neural networks. *Medical Image Analysis* **64**, 101751 (2020)
16. Sieren, J.P., Newell Jr, J.D., Barr, R.G., Bleecker, E.R., Burnette, N., Carretta, E.E., Couper, D., Goldin, J., Guo, J., Han, M.K., et al.: Spiromics protocol for multicenter quantitative computed tomography to phenotype the lungs. *American journal of respiratory and critical care medicine* **194**(7), 794–806 (2016)
17. Tan, Z., Feng, J., Zhou, J.: Sgnet: Structure-aware graph-based network for airway semantic segmentation. In: *International Conference on Medical Image Computing and Computer-Assisted Intervention*. pp. 153–163. Springer (2021)
18. Wang, M., Jin, R., Jiang, N., Liu, H., Jiang, S., Li, K., Zhou, X.: Automated labeling of the airway tree in terms of lobes based on deep learning of bifurcation point detection. *Medical & Biological Engineering & Computing* **58**(9), 2009–2024 (2020)
19. Yun, J., Park, J., Yu, D., Yi, J., Lee, M., Park, H.J., Lee, J.G., Seo, J.B., Kim, N.: Improvement of fully automated airway segmentation on volumetric computed tomographic images using a 2.5 dimensional convolutional neural net. *Medical image analysis* **51**, 13–20 (2019)
20. Zhao, T., Yin, Z.: Airway anomaly detection by prototype-based graph neural network. In: *International Conference on Medical Image Computing and Computer-Assisted Intervention*. pp. 195–204. Springer (2021)
21. Zhao, T., Yin, Z., Wang, J., Gao, D., Chen, Y., Mao, Y.: Bronchus segmentation and classification by neural networks and linear programming. In: *International Conference on Medical Image Computing and Computer-Assisted Intervention*. pp. 230–239. Springer (2019)

# Supplementary Material for BronchusNet: Region and Structure Prior Embedded Representation Learning for Bronchus Segmentation and Classification

ID 588

Anonymous

**Table 1. Details of the BRSC: a benchmark for bronchus segmentation and classification.** The BRSC contains 100 cases of thoracic CT scans, where 60 cases are obtained from the public databases EXACT’09 & LIDC-IDRI, and 40 cases are collected from our cooperate hospital. The process of data acquisition and investigation follows the principles outlined in the declaration of Helsinki.

Dataset Attributes	Values
Size of axial slices	$512 \times 512$
Thickness of axial slices	0.75mm $\sim$ 1.00 mm
Number of the cases in BRSC	100
Number of the cases from EXACT’09	20
Number of the cases from LIDC	40

**Table 2. Sensitivity analysis on the hyper-parameter  $\alpha$  of the neighborhood consistency regularization (NCR).** The NCR term is weighted by  $\alpha$  to make a trade-off between the cross-entropy loss and the NCR, as shown in Eq (5) in the paper. When  $\alpha = 0$ , the result is the same as the baseline. As  $\alpha$  becomes larger, the accuracy of our model first increases then decreases. Setting  $\alpha$  to 1 shows the highest accuracy.

$\alpha$	0	0.5	1	1.5	2
Accuracy	$92.0_{\pm 0.01}$	$92.8_{\pm 0.01}$	$93.1_{\pm 0.01}$	$92.5_{\pm 0.01}$	$92.1_{\pm 0.01}$

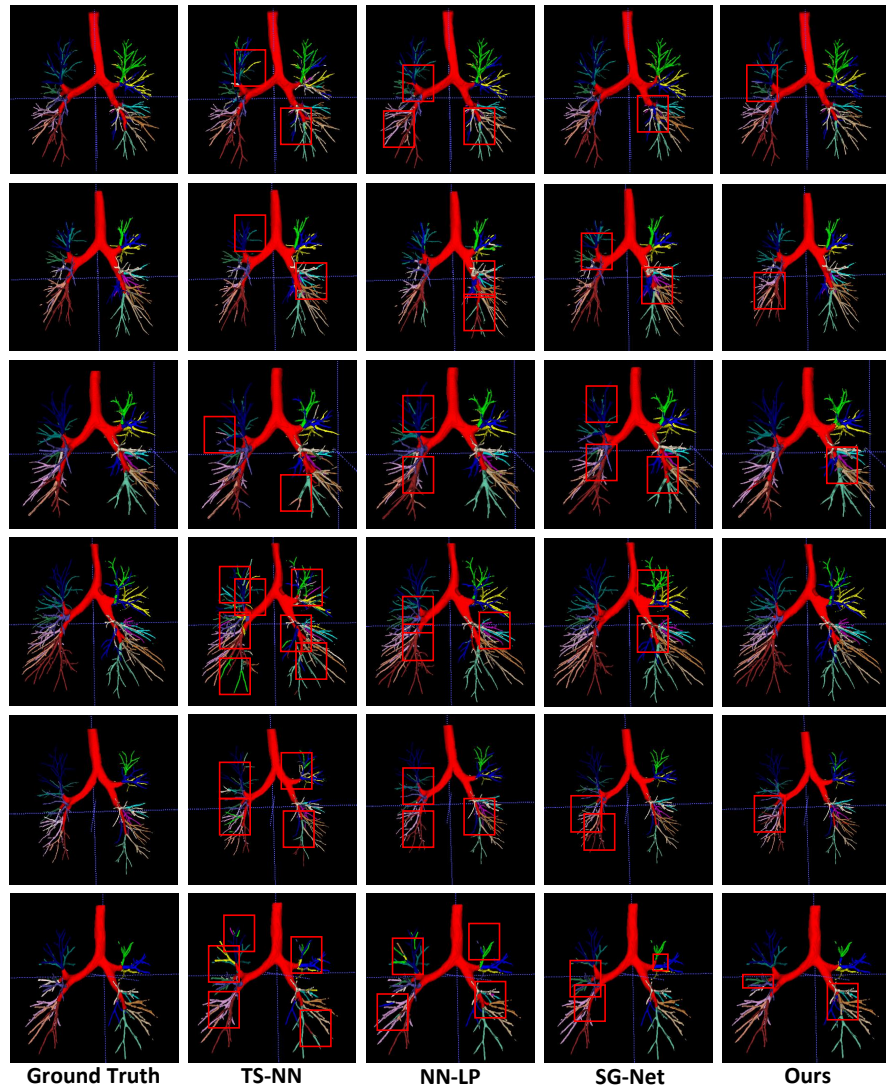


**Fig. 1.** Visualization results of the proposed method and other state-of-the-art methods. The misclassified bronchus is bounded by a red-line box. As we can see, the proposed BronchusNet exceeds other methods and shows more spatially coherent results in most cases.